行政院國家科學委員會專題研究計畫　期中進度報告

彈性體機器蛇之設計與導航(1/2)

計畫類別： 個別型計畫
計畫編號： NSC93-2212-E-002-051-
執行期間： 93 年 08 月 01 日至 94 年 07 月 31 日
執行單位： 國立臺灣大學生物產業機電工程學系暨研究所

計畫主持人： 周瑞仁

報告類型： 精簡報告
報告附件： 出席國際會議研究心得報告及發表論文
處理方式： 本計畫可公開查詢

中　華　民　國 94 年 5 月 30 日

行政院國家科學委員會補助專題研究計畫■精簡報告

Design and Navigation of a Snake Robot with a Flexible Body(1/2)

彈性體機器蛇之設計與導航(1/2)

計畫類別：■ 個別型計畫　　□ 整合型計畫

計畫編號：NSC 93－2212－ E －002－051－

執行期間：93 年 08 月 01 日至 94 年 07 月 31 日

計畫主持人：周瑞仁

共同主持人：

計畫參與人員：林振翔、王人毅

成果報告類型(依經費核定清單規定繳交)：■精簡報告　□完整報告

本成果報告包括以下應繳交之附件：

□赴國外出差或研習心得報告一份

□赴大陸地區出差或研習心得報告一份

□出席國際學術會議心得報告及發表之論文各一份

將參加 2005 年七月二十四日至二十八日舉辦的 IEEE/ASME International conference on advanced intelligent mechatronics, Monterey, CA, USA 並發表論文。待會議結束之後再繳交出席會議之心得報告

□國際合作研究計畫國外研究報告書一份

處理方式：除產學合作研究計畫、提升產業技術及人才培育研究計畫、列管計畫及下列情形者外，得立即公開查詢

□涉及專利或其他智慧財產權，□一年□二年後可公開查詢

執行單位：國立台灣大學生物產業機電工程學系

中　華　民　國　九十四 年　五 月　二十 日

Design and Navigation of a Snake Robot with a Flexible Body(1/2)

彈性體機器蛇之設計與導航(1/2)精簡報告

NSC 93-2212-E-002-051

Abstract—In this research, a snake robot with flexible connectors and distributed control system was developed and velocity planning was also investigated under the constraints of path, kinematics and the dynamics of the robot. The robot includes five modules which are connected by flexible springs. Each module is driven by two motors and controlled in a differential way for its direction and speed and coordinated and controlled by five microcontrollers. The flexible connectors make the robot's motion smoother and more snake-like in its movement. However, the elastic restoring force and torque, due to longitudinal extension or compression, and lateral bending of springs greatly affect the behavior of the snake robot's movement. A properly designed and controlled snake robot with a camera could track the planned path accurately and smoothly without sliding and losing steps.

Keywords: Snake robot, dynamics, microcontrollers, velocity planning

摘要—本研究研發一具有彈性連結器與分散式控制系統之機器蛇，並探討其於運動與動力學條件限制下的路徑與速度規劃模式。此機器蛇包含五個模組，模組間以彈簧連結，而每個模組各由兩個馬達以差動的方式決定其速度與方向。整體系統係受五個微控制器的協調與控制。彈性連結器使得機器蛇的動作的確蜿蜒逼真似蛇，惟彈性體的延伸與壓縮所造成的恢復力與力矩卻影響機器蛇之運動甚劇。因此適當設計與控制並裝有攝影機的機器蛇方能依所規畫的路徑行走而不致於打滑或失步。

關鍵字：機器蛇，動力學，微控制器，速度規畫

Introduction

Snake robots, imitating these features, are able to move in the surroundings of limited space, through various terrains or around multiple obstacles. These abilities make snake robots suitable for such work as rescue or collecting information in disaster areas. Therefore, the development of snake robots is an important and valuable research issue.

In this research, a snake robot with flexible connectors was developed. Its main characteristics are a flexible and slender body. These features make the movement of the snake robot much like that of a living snake. The path used in this research is simply composed of arcs and straight lines to avoid obstacles. The camera was implemented to identify the environment and spring deflections.

Methods and Materials

The snake robot developed in this research was composed of five modules connected by four 15cm long flexible springs (Fig.1).

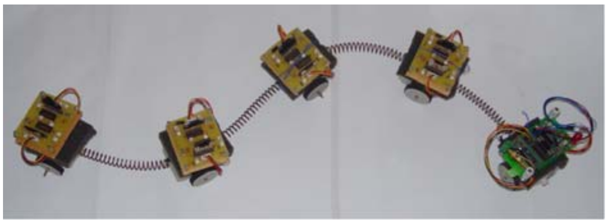

Fig. 1. Skelton of the developed snake robot.

Each module is composed of a POM (PolyOxyMethylene) casing, two stepper motors, counter weights, reduction gears, wheels and tires. Volume and weight for the modules are major concerns of the design. If the volume of the modules is too large, obstacle avoidance becomes more difficult. However, if the weight is too low, not enough friction will be created to drive the module. Therefore, a counter weight was designed to adjust the weight of the module. The weight of the module without the wheels is 620g, and the dimensions are 70(L) x 58(W) x 50(H) in mm.

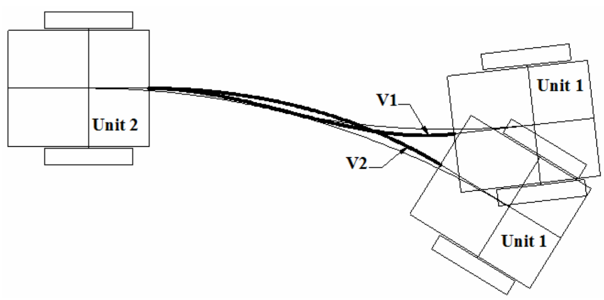

Fig. 2. The shape of springs approximated by NURBS

The casing and wheels were also made from POM (Polyoxymethylene), which features high temperature resistance up to 120°C. The tires were mounted on wheels, which were made from EPDM (Ethylene Propylene Diene Monomer) which features a high friction coefficient.

Uni-polar stepper motors were adopted in this study. The maximum suggested operating temperature for these motors is 80°C. The temperature and output torque of the stepper motors are related to working frequency, voltage and exciting method. To avoid any high temperature occurring in the casing, we set the operating voltage of the stepper motor at 18V with 1-1 phase exciting. The stepper motors were controlled by a micro controller through the signals amplified by Darlington pairs.

The velocity of the robot should be carefully planned under the constraints of kinematics and dynamics to ensure that no sliding or losing steps occur. In addition to longitudinal compression or extension, lateral bending is needed and must be considered in this study. The shape of the spring depends on the position and orientation of each module. Different shapes of the spring results in different restoring forces and torque.

The relationship between operating frequency and maximum output torque is nonlinear. To facilitate the dynamic analysis, the data were fitted by a six-order polynomial to give a smoother curve as indicated by Eq. (1), where τ and Q are referred to output torque and operating frequency respectively.

$$\begin{aligned}\tau_{max} &= \tau(Q) \\ &= 3.065\times10^{-9}Q^6 - 3.289\times10^{-6}Q^5 + 1.451\times10^{-3}Q^4 \\ &\quad - 0.337Q^3 + 43.283Q^2 - 2921.2Q + 81082\end{aligned} \quad (1)$$

According to Lee's study, the planned path is simply composed of arcs and straight lines. When the modules move in a straight line, the compression or extension of springs can be calculated by the speed of the modules. However, if the modules move in a curved line, the spring will bend and generate lateral restoring force and torque on the modules.

The shape of the spring can be expressed approximately by a spline curve, where a 2nd or 3rd order NURBS (Non-Uniform Rational B-Spline) curve was employed to approximate the shape of spring. The parameters needed to form a NURBS curve include coordinates and tangent direction at both end points of the springs. Eq. (2) shows the NURBS curve equation, P(u). In the equation, there are n+1 points. V_i refers to the control points, W_i refers to the weighting for each control point, *k* indicates the order of NURBS curve and $N_{i,k}(u)$ is the basis functions.

$$P(u) = \frac{\sum_{i=0}^{n} N_{i,k}(u) W_i V_i}{\sum_{i=0}^{n} N_{i,k}(u) W_i} \quad (2)$$

Fig. 2 shows the shape of springs simulated by 2^{nd} and 3^{rd} order NURBS curves V1 and V2 separately.

In order to verify the fitness, two modules connected by a spring were tested and coincided with NURBS curves as illustrated in Fig. 2.

When the spring deforms it generates a longitudinal elastic restoring force F_P, lateral restoring force F_L and elastic restoring torque M_z. The elastic restoring forces and torque depend on the shape of the spring. They can be expressed by NURBS functions.

Elastic restoring forces and torques generated by springs are external, thus the resulting longitudinal force, lateral force and torque should be zero to keep a module from sliding or losing steps. Because the static friction force and output torque of motors are limited, it is necessary to plan the path of the snake robot properly. In this way, the elastic restoring force and torque can be kept from becoming too large, which may cause the module to slide, the wheels to become suspended or the stepper motors to lose steps. The dynamic analysis in this study was based on the following assumptions:

1) The two stepper motors in a module have the same characteristics; 2) The snake robot is moving in a 2D space; 3) Modules will not pitch around the w heel axis.

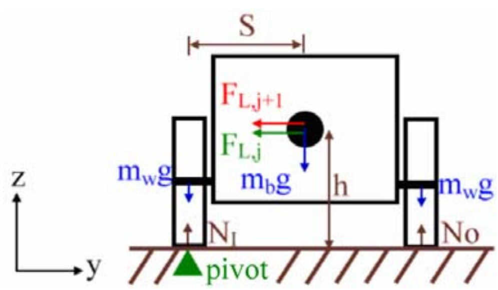

Fig. 3. Force acting on a module (Front view).

The lateral forces acting on each module include lateral elastic restoring forces $F_{L,j}$ and $F_{L,j+1}$ and lateral static friction forces f_{rLI} and f_{rLO}. The summation of these forces should be zero to keep the module from lateral sliding.

Lateral static friction force should be smaller than maximum static friction f_{rLmax} which depends on normal force N,.

As shown in Fig.3, normal forces of inside and outside wheels N_I and N_O (when the module moves in a curvilinear path) depend on lateral elastic restoring forces $F_{L,j}$ and $F_{L,j+1}$, which represent resultant force on the z axis and resultant torque on the x axis. These two equations can also be used to check if the wheel is suspended or not. (N_I=0 or N_O=0).

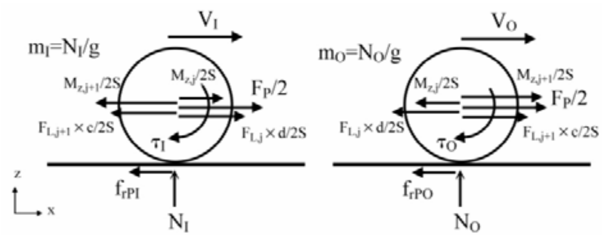

Fig. 4. Forces and torques acting on wheels (Side view).

In addition to lateral elastic restoring force, there are also longitudinal elastic restoring forces and torques acting on the module. These forces and torques will be converted to equivalent forces on the inside and outside wheels for analysis.

The summation of longitudinal elastic restoring forces is $F_p=F_{p,j}- F_{p,j+1}$ that inside and outside wheels share $F_p/2$ separately. The equivalent forces of lateral elastic restoring forces $F_{L,j}$ and $F_{L,j+1}$ are $F_{L,j}d/2S$ and $F_{L,j+1}c/2S$. The equivalent forces of elastic restoring torques $M_{z,j}$ and $M_{z,j+1}$ are $M_{z,j}/2S$ and $M_{z,j+1}/2S$.

The equivalent masses of wheels can be determined by the normal forces. In this way, the equivalent masses of the inside and outside wheels are N_I/g and N_O/g as shown in Fig. 4; where τ_I and τ_O refer to output torque of the motors, f_{rPI} and f_{rPO} represent longitudinal static frictions between the ground and the tire, respectively, and the radius of the wheels is r. The direction of static friction in Fig.4 is not always opposite to the moving direction of module. The direction of static friction depends on the external force of the module and torque of the motor.

Assuming the resultant external forces acting on the inside and outside wheels are F_I and F_O, as shown in Eqs. (3) and (4).

$$-\frac{\mathbf{M}_{z,j+1}}{2S}-\frac{\mathbf{F}_{L,j+1}\cdot\mathbf{c}}{2S}+\frac{\mathbf{M}_{z,j}}{2S}+\frac{\mathbf{F}_{L,j}\cdot\mathbf{d}}{2S}+\frac{\mathbf{F}_P}{2}=\mathbf{F}_I \tag{3}$$

$$-\frac{\mathbf{M}_{z,j}}{2S}-\frac{\mathbf{F}_{L,j}\cdot\mathbf{d}}{2S}+\frac{\mathbf{M}_{z,j+1}}{2S}+\frac{\mathbf{F}_{L,j+1}\cdot\mathbf{d}}{2S}+\frac{\mathbf{F}_P}{2}=\mathbf{F}_O \tag{4}$$

The longitudinal static friction force f_{rPI}, angular acceleration α_I and acceleration a_I of an inside wheel can be found by using Eqs. (5), (6) and (7), where I_I refers to the moment of inertia.

$$\mathbf{F}_I-\mathbf{f}_{rPI}=\frac{\mathbf{N}_I}{\mathbf{g}}\mathbf{a}_I \tag{5}$$

$$\tau_I-\mathbf{f}_{rPI}\cdot\mathbf{r}=\mathbf{I}_I\alpha_I \tag{6}$$

$$\mathbf{a}_I=\mathbf{r}\,\alpha_I \tag{7}$$

Eq. (6) can be rewritten as Eq. (8) which refers to the torque needed for acceleration and external force resistance. Output torque of the external wheel τ_O can be derived through the same procedure.

$$\tau_I = f_{rPI} \cdot r + I_I \alpha_I \quad (8)$$

Before planning the speed of the robot, it is necessary to plan the angular velocity of the inside and outside wheels of a module when moving on a path with varying curvature sections. The optimal angular velocity is determined by the radius of the arc sections of the path and the result of dynamic analysis. The planned optimal angular velocity allows the modules to follow the planned path in the shortest amount of time without the wheels sliding while preventing the stepper motor from losing steps.

The orientation and speed of a module are controlled by two wheels in a differential way. If both wheels rotate at the same angular velocity, the module moves in a straight line. Otherwise, the trajectory of a module is an arc line. The radius ρ and central angle θ of the arc are determined by a differential ratio ω_I/ω_o, where ω_I and ω_o indicate angular velocities of the inside and outside wheels respectively. The differential ratio ω_I/ω_o can be derived from the Eq. (9).

$$\frac{\omega_I}{\omega_O} = \frac{\rho - S}{\rho + S} \quad (9)$$

Once the optimal velocity is planned, based on the consideration of dynamics and kinematics, a different velocity, V_i, is obtained for every different section of the planned path, as shown in Fig. 5. To coordinate each modules of the robot, a minimum velocity at each section must be chosen.

Results and Discussion

In this study, an equivalent model for each module in ADAMS was built, and the validity of the dynamic analysis was verified.

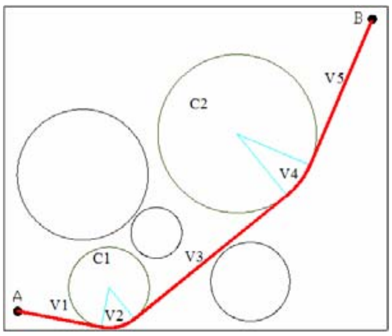

Fig. 5. Path sections with varying speed of wheels.

Testing was conducted with varying velocities and paths (Figs. 6 & 7) for the developed snake robot. In the velocity test, the speed of a module is proportional to the operating frequency. The overall relation is almost linear. Furthermore, the linear correlation is helpful for velocity planning.

Three paths were used in the test (Figs. 8): a straight line, arc and S shape curves. Springs were implemented as flexible connectors. We first employed sponge as a connector. Due to the reason that the sponge is elasto-plastic material, it is inherently nonlinear and therefore difficult to model and control. A small error in the initial positioning could cause the robot to slide or lose steps. By implementing spring into the design, the tracking performance was greatly improved.

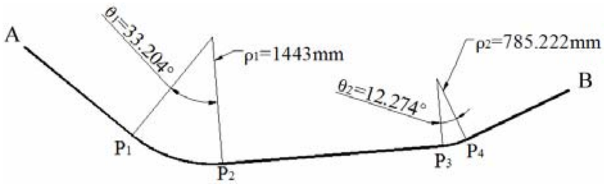

Fig. 6. Simulation path.

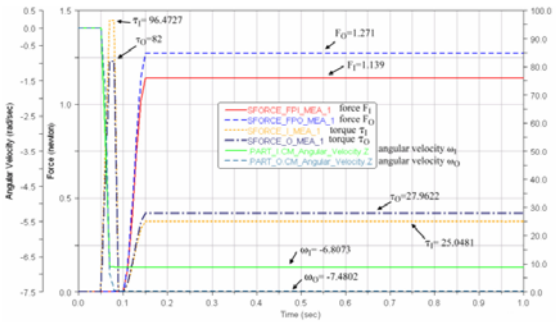

Fig. 7. Simulation result for the module situated on point P_3 of the path.

Fig. 8. Snake robot with springs as the flexible connectors.

Conclusion

In this study, the snake robot is designed to effectively attain the above mentioned results under the constraints of flexible connectors, planned paths, mechanisms and dynamics with the optimal speed planning method. Finally, this method is verified by the model built in ADAMS and field testing. The results show the robot will not slide or lose steps while moving according the speed planned by the method.